PNAS
www.pnas.org

Supplementary Information for

Acquirement of water-splitting ability and alteration of charge-separation mechanism in photosynthetic reaction centers

Hiroyuki Tamura, Keisuke Saito and Hiroshi Ishikita *

Hiroshi Ishikita
Email: hiro@appchem.t.u-tokyo.ac.jp

This PDF file includes:

Supplementary text
Figures S1 to S3
Tables S1 to S5
Legends for Datasets S1 to S2
SI References

Other supplementary materials for this manuscript include the following:

Datasets S1 to S2

www.pnas.org/cgi/doi/10.1073/pnas.2000895117

Supplementary Information Text

Stretch of the chlorin ring along the Qy transition dipole moment. From the observation of the PSII crystal structure (1), it seems likely that van der Waals contact of the Q_A isoprene side chain and P_{D1} make Chl_{D1} deformed along the Qx transition dipole moment, and make it stretched toward the Qy transition dipole moment. Indeed, removal of Q_A made the N…N distances of Chl_{D1} lengthened toward the Qx transition dipole moment and shorted toward the Qy transition dipole moment (Table S3). It should also be noted that this does not hold for PbRC, because the Q_B isoprene side chain, not the Q_A isoprene side chain, is oriented toward B_M.

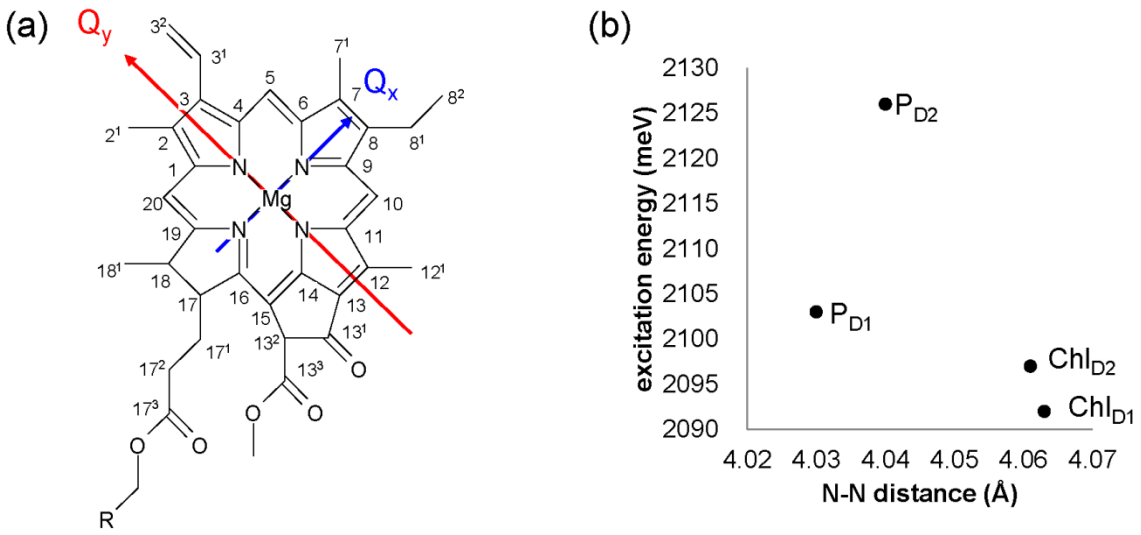

Fig. S1. (a) Orientations of the Qx and Qy transition dipole moments. (b) N…N distances along the Qy transition dipole moments in Å and excitation energies of P_{D1}, P_{D2}, Chl_{D1}, and Chl_{D2} in meV.

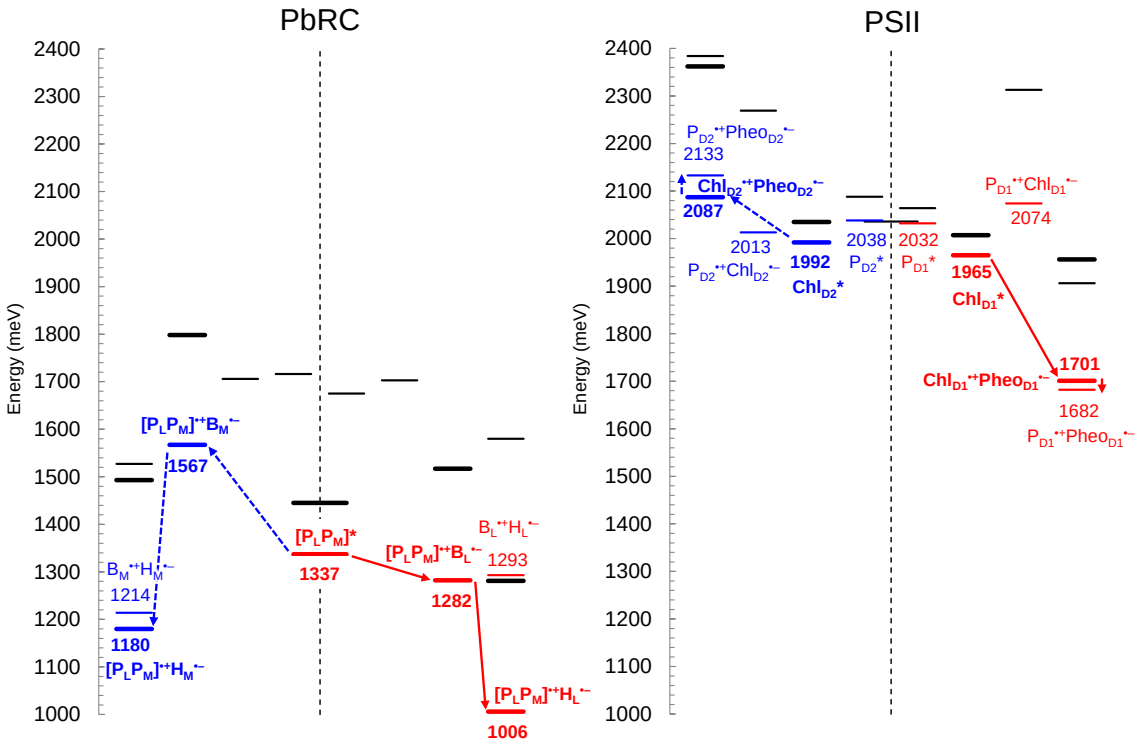

Fig. S2. Energy values for electronic excitation and charge-separated states of (B)Chl*a* and (B)Pheo*a* in PbRC (left) and PSII (right) in the presence of the intramolecular reorganization energy, calculated using a QM/MM approach, where the interaction between electron and hole was considered quantum-chemically. Thick solid bars indicate the major intermediate states. Red solid bars and arrows indicate major electron transfer in the active branch, and blue solid bars and dotted arrows indicate the corresponding electron transfer in the inactive branch.

Assuming that the excitation energy is 1424 meV (870 nm) for $[P_LP_M]$, the corresponding energies are 1766 meV (702 nm) for B_L, and 1763 meV (703 nm) for B_M based on Figure S2.

Assuming that the excitation energy is 1822 meV (680 nm) for Chl_{D1}, the corresponding energies are 1889 meV (656 nm) for P_{D1}, 1895 meV (654 nm) for P_{D2}, and 1849 meV (670 nm) for Chl_{D2} based on Figure S2.

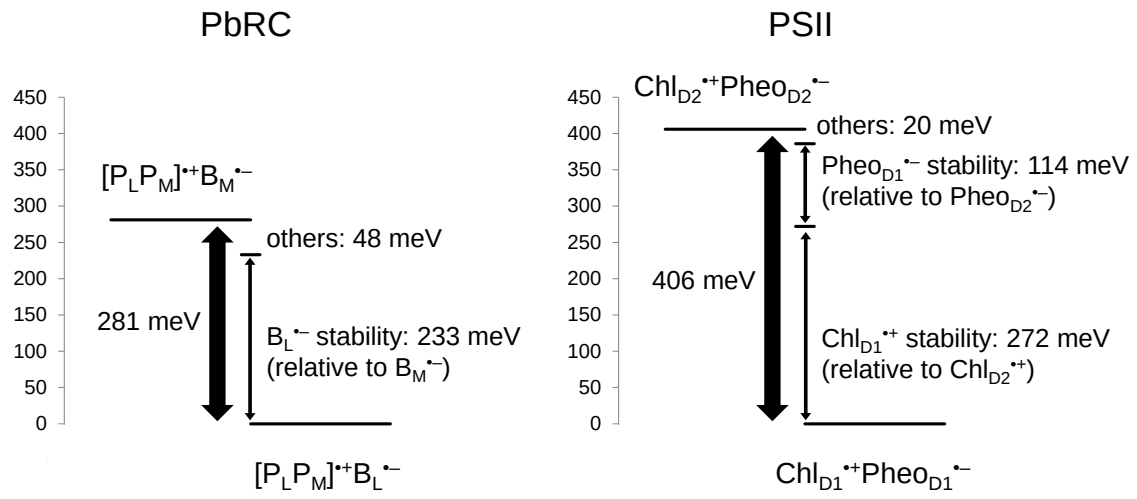

Fig. S3. Contribution of the cationic and anionic species to the energy difference in the charge-separated states between the active and inactive branches in meV.

Table S1. Coupling matrix for the [P_LP_M] bacteriochlorophyll pair in PbRC in meV. Values in brackets stand for the excited states calculated as the [P_LP_M] dimer bacteriochlorophylls in the PbRC protein environment. Note that values in Figure 2 were calculated as the P_L and P_M monomer bacteriochlorophylls, which are essentially the same as shown here.

	$\mathbf{P_L^*}$	$\mathbf{P_M^*}$	$\mathbf{P_L^{\bullet+}P_M^{\bullet-}}$	$\mathbf{P_L^{\bullet-}P_M^{\bullet+}}$
$\mathbf{P_L^*}$	(1673)	-27	-136	-113
$\mathbf{P_M^*}$		(1704)	-120	-138
$\mathbf{P_L^{\bullet+}P_M^{\bullet-}}$			(1739)	20
$\mathbf{P_L^{\bullet-}P_M^{\bullet+}}$				(1709)

Table S2. Coupling matrix for the [$P_{D1}P_{D2}$] Chl*a* pair in PSII in meV. Values in brackets stand for the excited states calculated as the [$P_{D1}P_{D2}$] dimer chlorophylls in the PSII protein environment. Note that values in Figure 2 were calculated as the P_{D1} and P_{D2} monomer chlorophylls, which are essentially the same as shown here.

	P_{D1}*	**P_{D2}***	**$P_{D1}^{\bullet+}P_{D2}^{\bullet-}$**	**$P_{D1}^{\bullet-}P_{D2}^{\bullet+}$**
P_{D1}*	(2051)	-10	9	10
P_{D2}*		(2071)	4	32
$P_{D1}^{\bullet+}P_{D2}^{\bullet-}$			(2140)	4
$P_{D1}^{\bullet-}P_{D2}^{\bullet+}$				(2590)

Table S3. N…N distances along the Qx and Qy transition dipole moments in the QM/MM-optimized geometry in Å.

	P_{D1}	P_{D2}	Chl_{D1}	Q_A-depleted Chl_{D1}	Chl_{D2}
Qx	4.184	4.243	4.151	4.167	4.191
Qy	4.030	4.040	4.063	4.057	4.061

Table S4. Residues and water molecules that decrease the excitation energy of Chl_{D1} and Chl_{D2} with respect to P_{D1} and P_{D2} in meV.

	P_{D1}	P_{D2}	Chl_{D1}	Chl_{D2}
D1-His198[a]	11			6
D2-His197[b]		10	7	
ligand H_2O for Chl_{D1}[c]			8	
ligand H_2O for Chl_{D2}[d]				10
H-bonding H_2O (W382D)[e]		3	15	
H-bonding H_2O (W349A)[f]	7			13
total	18	13	30	29

[a] Serving as a ligand residue for P_{D1} and an H-bond donor to W382D.
[b] Serving as a ligand residue for P_{D2} and an H-bond donor to
[c] W424D and the second sphere ligand W1003A.
[d] W1009A and the second sphere ligand W359A.
[e] Donating an H-bond to the Chl_{D1} keto group and accepting an H-bond from D2-His197.
[f] Donating an H-bond to the Chl_{D2} keto group and accepting an H-bond from D1-His198.

Table S5. L/M residue pairs that stabilize $H_L^{\bullet-}$ with respect to $H_M^{\bullet-}$ (>40 meV) in the LUMO energy level in meV, i.e., corresponding to E_m for one-electron reduction.

	$E_m(H_L)$	$E_m(H_M)$		$E_m(H_L)$	$E_m(H_M)$	stabilizing $H_L^{\bullet-}$
Glu-L104	128	3	Thr-M133	0	8	117
Asp-L218	-8	-54	Trp-M254	-3	0	43
Tyr-L67	3	0	Glu-M95	-8	-46	41

Dataset S1 (separate file). QM/MM-optimized atomic coordinates for PbRC.

Dataset S2 (separate file). QM/MM-optimized atomic coordinates for PSII.

References

1. Umena Y, Kawakami K, Shen J-R, & Kamiya N (2011) Crystal structure of oxygen-evolving photosystem II at a resolution of 1.9 Å. *Nature* 473:55-60.